PCCP

Cite this: *Phys. Chem. Chem. Phys.*, 2012, **14**, 16250–16257

www.rsc.org/pccp

PAPER

Complex design of dissipation signals in non-contact atomic force microscopy

J. Bamidele,[a] Y. J. Li,[b] S. Jarvis,[c] Y. Naitoh,[b] Y. Sugawara[b] and L. Kantorovich*[a]

Received 6th September 2012, Accepted 18th October 2012
DOI: 10.1039/c2cp43121a

Complex interplay between topography and dissipation signals in Non-Contact Atomic Force Microscopy (NC-AFM) is studied by a combination of state-of-the-art theory and experiment applied to the Si(001) surface prone to instabilities. Considering a wide range of tip–sample separations down to the near-contact regime and several tip models, both stiff and more flexible, a sophisticated architecture of hysteresis loops in the simulated tip force–distance curves is revealed. At small tip–surface distances the dissipation was found to be comprised of two related contributions due to both the surface and tip. These are accompanied by the corresponding surface and tip distortion approach–retraction dynamics. Qualitative conclusions drawn from the theoretical simulations such as large dissipation signals (>1.0 eV) and a step-like dissipation dependent on the tip–surface distance are broadly supported by the experimental observations. In view of the obtained results we also discuss the reproducibility of NC-AFM imaging.

Introduction

Damping in non-contact atomic force microscopy (NC-AFM) corresponds to energy dissipation in the cantilever–sample system (the amount of additional energy required for the oscillating cantilever to maintain a constant amplitude at resonance.) This phenomenon has been most effectively explained by the adhesion hysteresis mechanism, whereby atomic relaxations in the junction (*i.e. both* in the tip and sample) on approach and retraction differ,[1–6] leading to the tip and surface atoms following two different trajectories and hence to the tip force hysteresis (two different force *vs.* distance (f–z) curves). However the debate about the mechanism is still somewhat open.[4,7–10]

Typically dissipation of the order of 0.01–1 eV per oscillation (p/o) cycle is experimentally measured at stable imaging conditions,[1,6] but signals exceeding 1 eV p/o (and up to 10 eV p/o) have also been reported.[11,12] Recently, theoretical studies have made tremendous contributions to our understanding of what causes dissipation and in answering the question of why and how it provides atomic contrast. However, these studies have been mostly limited to either ascertaining the dominant mechanism behind dissipation (*e.g.* one or a few atoms of the surface jumping up to the tip then returning to the surface upon tip retraction) or interpreting dissipation signals. Dissipation effects were also discussed in the context of manipulation with the AFM probe.[13–16] At the same time, there has been little discussion on the architecture behind the individual signals that are averaged over in experimental measurements because of the tip oscillations, and the complexities related to contrast changes as a function of the tip–sample distance for systems where no atomic depositions or removals occur. A discussion on the dissipation behaviour as the function of the tip–sample distance was presented in ref. 17 in the context of pulling a chain of atoms from the tip. Moreover, no study has previously been done at the *near-contact* regime alongside a discussion as to whether this can still lead to reproducible atomic contrast both in topography and dissipation.

In this paper we present a detailed theoretical study on the complex architecture that may be behind observed dissipation signals. Main conclusions are broadly supported by experimental results.

Using state-of-the-art *ab initio* density functional theory (DFT) we meticulously examine the nature of dissipation up to the near-contact regime. We focus on tracking the changes in dissipation signals as a function of the tip–sample separation and lateral position of the tip, revealing the complexities behind these changes. We go on to characterize the atomistic processes that can lead to extremely large dissipation signals (>1 eV) in great detail. Then based on preliminary experimental results, which show sharp contrast and discontinuous intensity changes in the profiles of observed dissipation signals, we qualitatively confirm our theoretical conclusions.

We study the Si(001) surface,[18–21] chosen due to its known dissipative behavior when scanned using NC-AFM. Although it is now generally accepted that its low temperature (<120 K)

[a] *Department of Physics, King's College London, The Strand, London, WC2R 2LS, UK. E-mail: lev.kantorovitch@kcl.ac.uk*
[b] *Department of Applied Physics, Osaka University, 2-1 Yamada-oka, Suita, Osaka 565-0871, Japan*
[c] *The School of Physics and Astronomy, University of Nottingham, Nottingham, NG7 2RD, UK*

ground state geometry is the buckled dimer $c(4 \times 2)$ phase,[22–27] the $p(2 \times 2)$ phase is also observed in local surface areas[27] (see discussion in ref. 28 and 29). A possible channel by which dissipation is thought to occur in this surface is primarily due to the flipping of these dimers.[24] We shall see that this is generally true only for not very close approaches; more complex dissipation mechanisms involving the atoms at the tip apex as well are at work if the tip comes very close to the surface, especially in the near-contact or even contact regimes. In our study we use silicon tips, effectively avoiding effects due to different atomic species. Thus, this system allows for thorough scrutiny of only the mechanical tip–sample processes that occur.

Methods

To study dissipation in this system, we have performed extensive *ab initio* DFT calculations carried out using the localized basis set code SIESTA,[30] utilizing periodic boundary conditions, double-zeta polarized basis set and norm-conserving pseudopotentials. We used the generalized gradient approximation (GGA) density functional as employed by Perdew–Burke–Ernzerhof (PBE)[31] and a single Gamma ($k = 0$) k-point sampling. The surface was modeled by an eight-layer slab with a cell containing eight dimers arranged in two rows with four dimers in each row; the bottom four layers were frozen in the bulk geometry and unsaturated bonds at the bottom of the slab were terminated with hydrogen atoms; the four uppermost layers of the slab were allowed to relax. Two tip models were used: (i) a relatively stiff standard 25 atom pyramidal Si(111) cluster with a single dangling bond[25,32] in which only 4 apex atoms were allowed to relax, and (ii) a much more flexible dimer tip[27,33] containing 48 atoms with 15 atoms at its apex allowed to relax. In all our calculations, forces on the atoms which were moveable were typically converged to 0.01 eV Å^{-1}. The distance between the tip apex atom (the closest to the surface when the tip is far away) and the surface upper dimer atom *prior to relaxation* was used to measure the tip–surface separation.

Initially the unrelaxed distance between the tip apex and the upper dimer atom underneath was set to 0.7 nm. Using increments of 0.01 nm, this separation was then reduced to a minimum distance of 0.02 nm, corresponding to the very near-contact regime, and then retracted back to 0.7 nm using the same increments. After each change of the tip–sample separation, the system was allowed to fully relax. Such small increments were chosen to accurately capture any point where deviations occurred between the approach and retraction f–z curves. Retraction calculations were performed in a very specific way in order to capture *all possible* hysteresis loops. Firstly, the separation distance where the retraction curve deviated from the approach (if this occurs) was noted. Then using the relaxed structure of the system corresponding to the point on the *approach curve*, which was at a slightly larger tip–sample separation, a separate retraction was started. This ensures that upon retraction the approach curve will be followed until the next point of deviation (if any). This process of retraction was done until a 0.7 nm tip–sample separation so that all deviations were accounted for. By performing the calculations in this way, we were able to calculate all the complete sets of hysteresis loops in the f–z curves for a number of sites along the line across a dimer. The dissipation was calculated as the area enclosed by the hysteresis loop(s).

In order to calculate the frequency shift curves and correspondingly the scan lines, which can be compared with experiment, a contribution due to macroscopic interactions with the surface (the van der Waals force) was added to the DFT calculated tip force using a spherical tip model.[34,35] This was achieved by using the analytical expression for a driven one-dimensional harmonic oscillator acting within an external field. This is the same model used in ref. 36, where a tip radius of 100 Å and an offset of +3 Å was employed for the pyramidal tip. The positive value for the offset was an initial indication that a larger tip model was required for more quantitatively accurate results, which when used (dimer tip) required an offset of only +1.7 Å. Generally, it was found that the effect the van der Waals contribution to the force had on the results was small and did not change the qualitative results. Note that an average tip force over the whole oscillation cycle was required to be used in calculating the frequency shift in cases when the tip force demonstrates a hysteric behaviour.

The experiment was performed with a home-built NC-AFM operated in ultra-high vacuum (UHV) at a low-temperature.[28] The deflection of the cantilever was detected by an optical fiber interferometer, one of the most sensitive deflection sensors. The frequency-modulation technique[29] was used with a commercial silicon cantilever (Nanosensors, type NCLR-W) as a force sensor, with 40 N m^{-1} spring constant and 171 kHz resonance frequency (n-type, Sb-doped Si wafer). In order to remove the native oxide layer and any contamination on the tip, the cantilever was cleaned by Ar^+ ion sputtering, and hence the tip apex is likely to be terminated by dangling bonds. As a sample, an As-doped n-type Si(001) wafer with a conductivity of 0.01–0.025 Ω cm was used. The sample was cleaned by repeated cycles of flashing at 1200 °C and annealing at 950 °C after pre-baking for one night (over 12 hours). All measurements were performed at 5 K. Topographic images were measured from the feedback signal for the distance control between the tip and the sample at a constant frequency shift Δf and at a constant oscillation amplitude $A = 13.5$ nm. Dissipation images were obtained simultaneously with the topography during the scanning. Both the cantilever and the sample were always electrically grounded to 0 V.

Results

We start by discussing the results of our theoretical calculations with the stiffer tip. A complete set of approach and retraction simulations performed as described above is shown in Fig. 1, for the tip positioned above a site close to the lower dimer atom (position 5 in Fig. 3(b)).

As shown in Fig. 1(a), if the tip closest approach, d, during oscillations is not closer than 0.26 nm, it follows the same path upon retraction producing no dissipation. Closer approaches to about 0.17 nm, Fig. 1(d), results in a different retraction path up to 0.5 nm (a hysteresis loop). Therefore for tip oscillations with d anywhere between 0.17–0.26 nm, a fixed dissipation is observed, corresponding to a dimer flipping event, as depicted in Fig. 1(e) and (f).

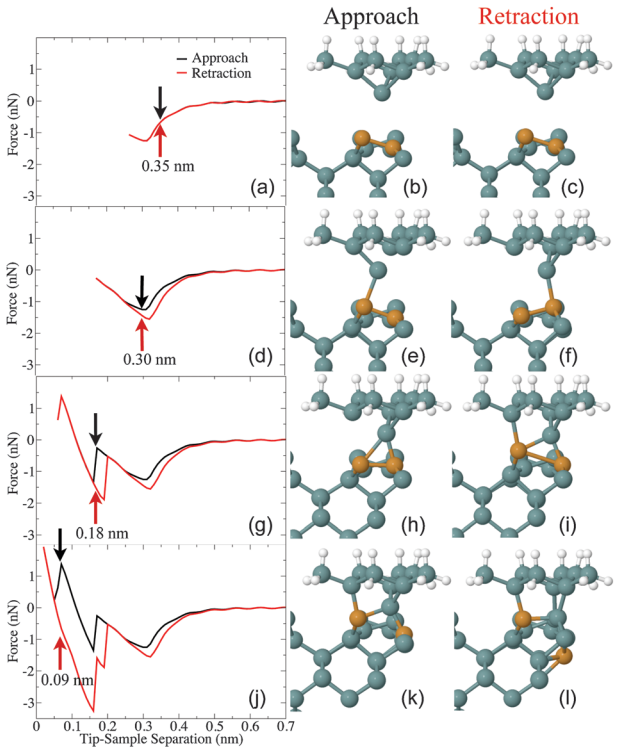

Fig. 1 Left panels: four pairs of theoretical approach (black) and retraction (red) *f*–*z* curves for different tip–sample separations, corresponding to the pyramidal tip positioned as in (b). The curves correspond to different minimum tip–sample separations on the approach, before the retractions were made, of: (a) 0.26 nm, (d) 0.17 nm, (g) 0.06 nm, and (j) 0.02 nm. Right panels: for each set of curves the corresponding geometries for characteristic tip–sample separations on the approach and retraction (indicated by arrows on the left panels) are shown. Turquoise and white balls depict Si and H atoms, respectively, while orange balls depict the two dimer atoms underneath the tip.

It should be noted that in our *static* zero temperature calculations, when the tip is removed after flipping the dimer, a three-in-a-row conformation of the surface dimers remains (illustrated in Fig. 2), composed of three Si dimers flipped in the same way. This is not observed experimentally and has previously[26,27] been explained by the fact that the three-in-a-row structure is mechanically unstable and the system eventually returns to the original conformation of alternating dimers characteristic for the $c(4 \times 2)$ reconstruction even at 5 K. Therefore, as soon as the dimer on a pristine Si(001) surface flips, it will flip back upon tip retraction. Although this is not captured in our static calculations, this feature affects neither the results nor their interpretation.

For *d* values between 0.06–0.17 nm, Fig. 1(g), a second hysteresis loop is observed which is due to the dimer being forcefully flipped back as the tip apex pushes back down the lower dimer atom, Fig. 1(h) and (i), leading to greater dissipation. At this point the tip bonds to several surface atoms and is noticeably distorted. At *near-contact* with the surface, with *d* between 0.02–0.06 nm, a third and significantly larger hysteresis loop is revealed, Fig. 1(j). Here the repulsion due to the lower dimer atom, now pushed back into the surface, increases, forcing it to go further into the surface, Fig. 1(k) and (l). Hence we see two dimer flipping events for a single approach. Upon retraction, the tip is completely restored and large dissipation occurs as a result of reversing all of the processes described, breaking several bonds. Interestingly, if retracted from any distance between 0.02–0.06 nm, the second hysteresis loop was found to join the third.

Note that the specific behavior of the dissipation signal, which remains the same over some interval of tip–sample distances and changes abruptly beyond that, results in a step-like dependence of dissipation on the tip height (at zero temperature).

These types of calculations were performed for seven lateral positions taken along a line passing through a dimer, as shown in Fig. 3(b). In our simulations, upon retraction of the tip, both the tip and sample nearly always regain their original geometries. This shows the tip and sample are not permanently deformed, indicating the results are reproducible over many oscillations, as they should be to produce clear experimental images. For some lateral positions, at near-contact, the atomic forces were large enough to displace the tip-terminating atom; once displaced, the lower dimer atom springs back up, and due to the presence of the rest of the tip, the dimer immediately

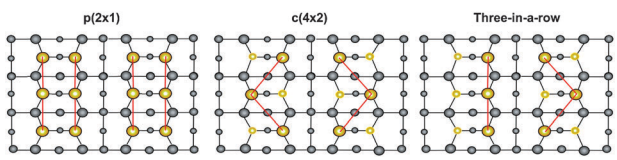

Fig. 2 Ball models of the $p(2 \times 1)$, $c(4 \times 2)$ and three-in-a-row reconstructions of the Si(001) surface.

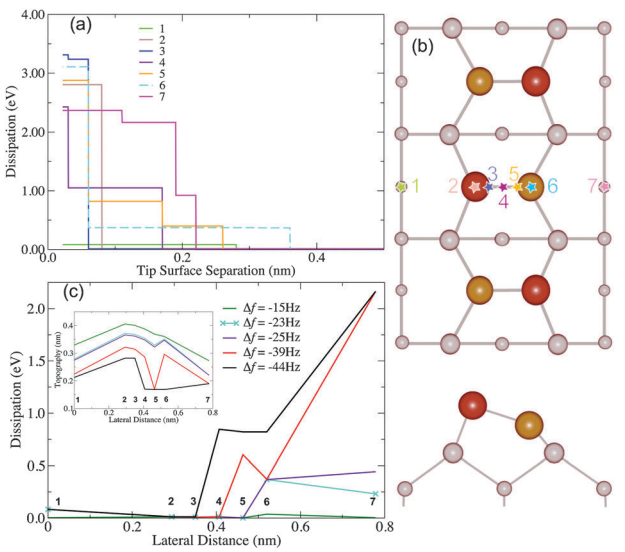

Fig. 3 Theoretical results: (a) Dissipation signal as a function of the pyramidal tip–sample separation for seven points along a dimer indicated in (b) using the same colour code. (c) Dissipation scan lines across a dimer for constant Δf values ranging from −15 Hz to −44 Hz, *i.e.* corresponding from 'very weak' to 'extremely strong' tip–sample interaction strengths. Inset is the corresponding topographic scan lines for the same frequency shift values, employing the same colour code. The numbers in the dissipation spectroscopy (a) and all scan line images (c) corresponds to the lateral positions numbered along the dimer shown in (b).

goes into its flipped conformation, *i.e.* in some cases up to three dimer flipping events occur during a single oscillation. The general trend that can be deduced from these calculations is that the tip interacts more strongly with the lower dimer atom than the upper dimer atom, forming and destroying more bonds, for larger tip–sample separations. This results in more dissipation measured over the lower dimer atom region for a wider range of Δf values than over the upper dimer atom region.

Dissipation spectroscopy curves using an oscillation amplitude of 13.5 nm are shown in Fig. 3(a) for the seven lateral positions, numbered in (b). It can immediately be seen, that for the region including the lower dimer atom (points 4–7), not only does the onset of dissipation occur at larger separations than for the other lateral positions 1–3 (corresponding the the area around the upper dimer atom), as we would expect (due to its affinity for flipping), but the magnitude increases in a discontinuous step-like manner, as more processes begin to contribute to the total dissipation signal as was explained above. The scan lines in Fig. 3(c) is an alternative method of representing the data in Fig. 3(a), best suited for a comparison with experimental images.

To further aid comparison with experiment (see below) in Fig. 3(c) we have simplified our *qualitative* discussion by distinguishing five important regions of tip–sample separation: 'very weak', 'weak', 'strong' and 'very strong' tip–sample interactions. Additionally we have included an 'extremely strong' interaction region corresponding to the contact/near-contact regime. Over these regions theory predicts that for large separations (very weak interactions, dark green curve), almost no dissipation is measured and the topography shows the ground-state surface (Fig. 3(c), inset), as expected. Then for reducing separations, we observe increasing dissipation above the lower dimer atom (turquoise curve), gradually extending over the entire lower dimer atom region (purple, red and black curves).

Our theoretical model based on the stiff tip predicts a very large (over 3 eV) dissipation signal for some lateral positions at close approach. This must be an overestimation due to a rather crude tip model in which only four bottom atoms were allowed to relax. At close approaches more atoms of the tip must be affected which should yield softer reaction of the tip during contact with the surface and, hence, smaller dissipation. There are clear experimental indications[37] that Si tips terminated with a dimer are also realistic tip models. To verify this, calculations were also performed for a single lateral position using another much larger dimer tip containing 15 bottom atoms allowed to relax. The results are shown in Fig. 4 for the tip positioned above the upper dimer atom. Note that various tip orientations of the dimer tip with respect to the surface dimer are possible and these would affect the ability of the tip to manipulate the surface;[38] only one such position is considered here, shown in Fig. 4.

At large separations the tip 'feels' the presence of the dimer, but does not flip it, and so any retraction made from a minimum distance d of 0.25 nm will not lead to any hysteresis in the f–z curve. Reducing the separation past this, to d = 0.07 nm, leads to a small but significant hysteresis loop. This loop occurs due to the flipping of the surface dimer, which flips back upon tip retraction. In the case of the pyramidal tip, the

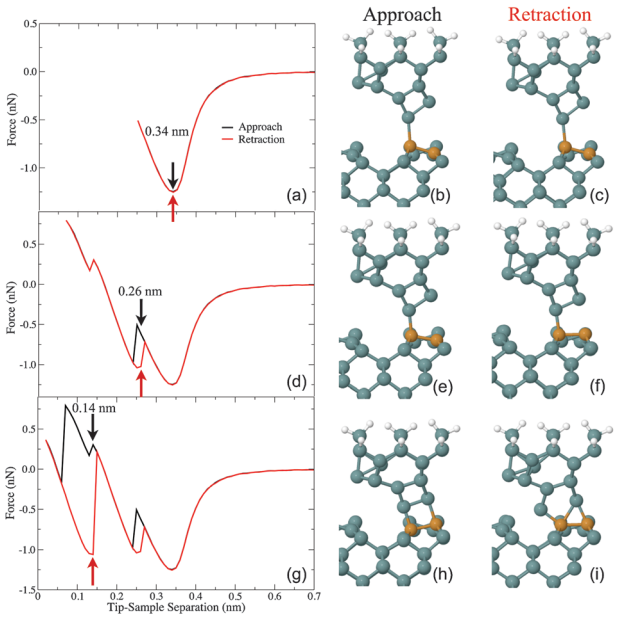

Fig. 4 Left panels: three pairs of theoretical approach (black) and retraction (red) f–z curves for different tip–sample separations, corresponding to the dimer tip positioned above the upper dimer atom (position 2 in Fig. 2(b)). The curves correspond to different minimum tip–sample separations on the approach, before the retractions were made, of: (a) 0.25 nm, (d) 0.07 nm and (g) 0.02 nm. Right panels: for each set of curves the corresponding geometries for characteristic tip–sample separations on the approach and retraction (indicated by arrows on the left panels) are shown. The colour scheme is as in Fig. 1.

flipping of the dimer when the tip is placed above the upper dimer atom/region was due to the very stiff apex forcing down the upper dimer atom(s). However, in the case of the dimer tip, due to the orientation of the tip, the dimer flips due to the upper dimer atom of the dimer apex bonding to the surface lower dimer atom. Then upon retraction, the surface dimer flips back to its original conformation due to the apex lower dimer atom being above the surface upper dimer atom (which was flipped into the lower position on approach), see Fig. 4(e) and (f). The formation/destruction of the bonds between the tip dimer apex and the surface dimer are shown as two sharp kinks in the f–z curve, Fig. 4(d).

A second a considerably larger hysteresis loop occurs for any retraction made from $d < 0.07$ nm. This results in considerably more dissipation being measured, and is due to the dimer apex being split apart by the surface dimer, Fig. 4(i). However, upon retraction of the tip, the dimer apex comes back together and the tip is fully restored. Therefore in this case dissipation occurs as a results of both the tip and surface atomic rearrangements, as well as the creation and destruction of tip–sample bonds.

Direct comparison between the two tip models for the dissipation signal as a function of the tip height for the lateral position above the surface upper dimer atom is shown in Fig. 5. It can immediately be seen that at separations above 0.07 nm our larger tip model predicts noticeable dissipation above the upper dimer atom whereas the small tip model predicts no dissipation at these distances, as follows from our discussion above and Fig. 3.

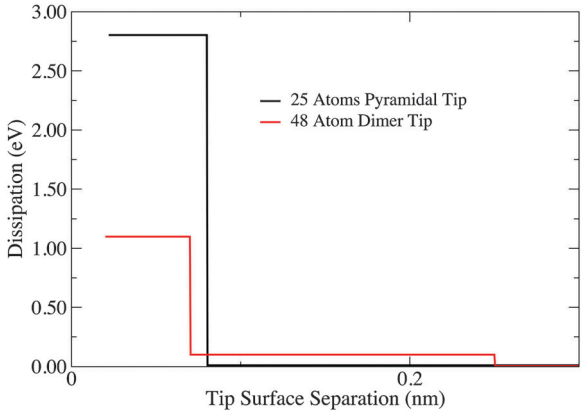

Fig. 5 Theoretically calculated dissipation signals as a function of tip–sample separation for the two tips (pyramidal, black, and dimer, red) positioned above the upper dimer atom.

At the same time, in the near contact regime ($d < 0.07$ nm) dissipation calculated with the dimer tip becomes very large (over 1 eV p/o). Importantly, however, this large and much more flexible tip predicts significantly smaller dissipation and softer contact (smaller tip force) than the stiffer pyramidal tip model – a result to be expected.

As seen from the detailed geometries along the approach–retraction cycles shown in Fig. 1 and 4 for the two tips, respectively, their geometries at the same height above the surface on approach and retraction are not the same for the values of d smaller than some critical height. This means that, as mentioned above, part of the calculated dissipation is due to the tip-related hysteresis alone.

To characterise this effect qualitatively, we extracted the vertical displacements of both tip apices and surface dimer atoms relative to their ideal positions (*i.e.* taken from their initial relaxed geometries when there was no tip–sample interaction), as a function of the tip–sample separation. This was done using the relaxed positions of tip and surface atoms from our full calculations along the approach–retraction cycle. We expect that since the dissipation is primarily due to the tip inducing surface dimer flipping and the creation/destruction of tip–sample bonds, the tip apex atom would experience hysteresis for the same range of values of d as the surface dimer. The results are shown in Fig. 6 and 7 for the pyramidal and dimer tips, respectively.

Interesting, observations of the role the tip plays in the dissipation effects can be seen when comparing the two tips. Much larger displacements occur within the more rigid pyramidal tip–sample system than within the dimer tip–sample system. Furthermore, two hysteresis loops form within the dimer tip–sample system (Fig. 7(a) and (d)), corresponding to when the lowest apex dimer atom bonds to the uppermost surface dimer atom (first loop at a larger tip–sample separation) and when the apex upper dimer atom bonds to the surface lower dimer atom (second loop). This, along with the observation that the magnitude of the hysteresis loops for the dimer tip–sample system is clearly significantly smaller than for the pyramidal tip-system, falls well in line with our expectations. In fact, the description of the mechanism behind the dissipation provided by this representation can be thought of as an

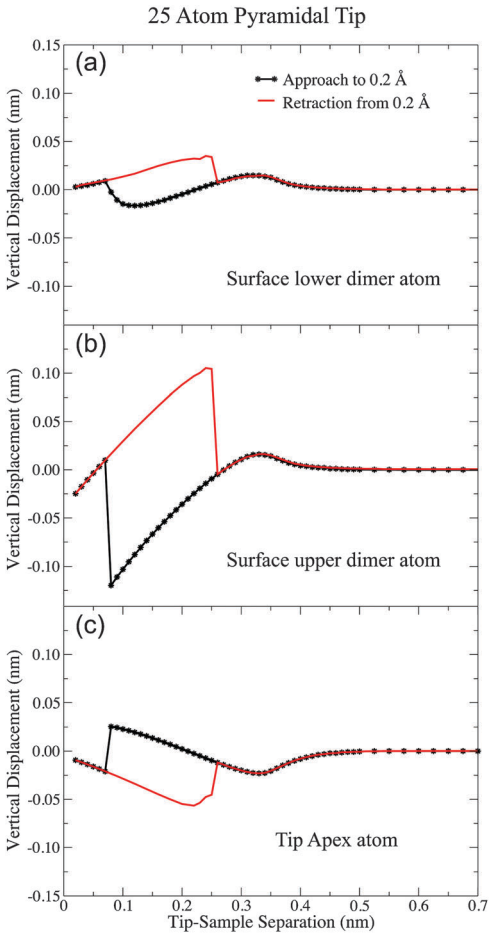

Fig. 6 Vertical displacements of the tip apex and surface dimer from their ideal positions as a function of tip–sample separation for the pyramidal tip.

alternative method to our f–z curves (considering only the major contributors to the dissipation), however, we now also simultaneously get some insight into the contribution of the tip to the overall dissipation. Thus, it follows from these results that the relaxation at the tip likely also contributes significantly into the overall dissipation effect. This is especially so for the dimer tip as hysteresis in the displacements of the tip apex is very similar in magnitude to those of the surface. This is not so much the case for the pyramidal tip–sample system where the tip displacements are much less than in comparison to the surface, albeit still a rather significant portion.

Summarising, theoretical calculations reveal that dissipation effects are very sensitive to the specific lateral position of the tip; it is much more difficult to induce a non-conservative distortion at the surface in stiff areas (like around the upper dimer atoms studied here), whereas softer regions (around lower dimer atoms) are much more susceptible to this kind of response. At the same time, if soft tips are more prone to non-conservative distortion than rigid ones, the actual dissipation energy may in the cases of rigid tips be still very significant as these are able to substantially deform the surface underneath.

These predictions of theory were tested with our preliminary experimental results performed at 5 K and presented in Fig. 8. We show results for four tip–sample interaction strengths,

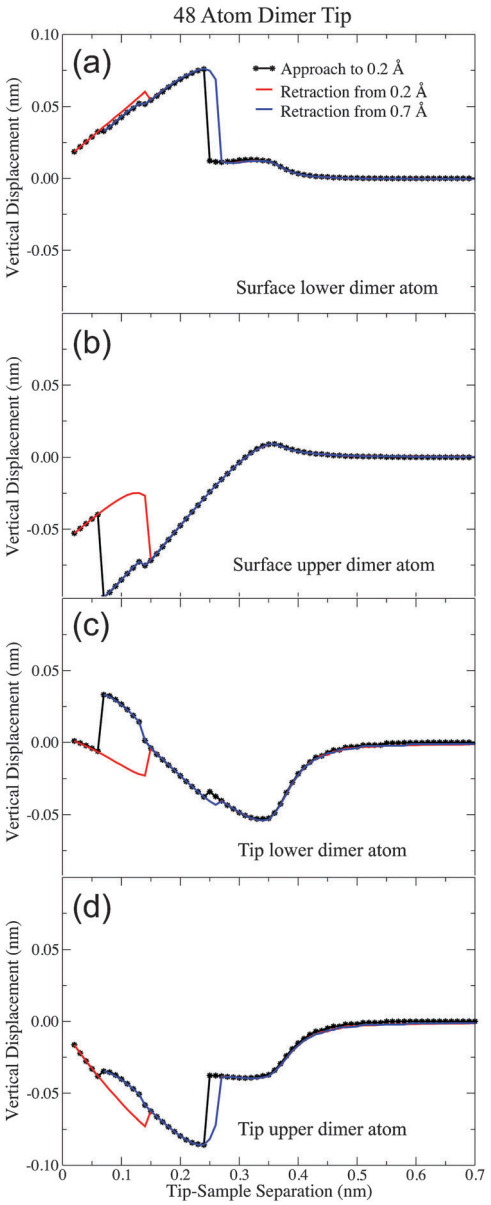

Fig. 7 Vertical displacements of the tip apex and surface dimer from their ideal positions as a function of tip–sample separation for the dimer tip.

ranging from very weak to very strong. Likewise with our theoretical calculations, we analyze the NC-AFM images and line scans taken along a dimer. When moving from left to right in Fig. 8, $|\Delta f|$ increases, so the average tip–sample distance decreases. In the case of very weak tip–sample interactions, when no manipulation of the surface by the tip is to be expected, shown in Fig. 8(a), the $c(4 \times 2)$ phase with zigzag pattern is observed in the topographic image (i, ii), with the upper dimer atom imaged higher than the lower dimer atom, corroborating that this phase is the ground state for this surface, while there is no information in the dissipation image (iv, v).

In the case of a weak tip–sample interaction, Fig. 8(b), the $c(4 \times 2)$ phase is clearly observed in both topographic and dissipation images, although these image patterns are different; the upper dimer atom still appears higher than the lower dimer

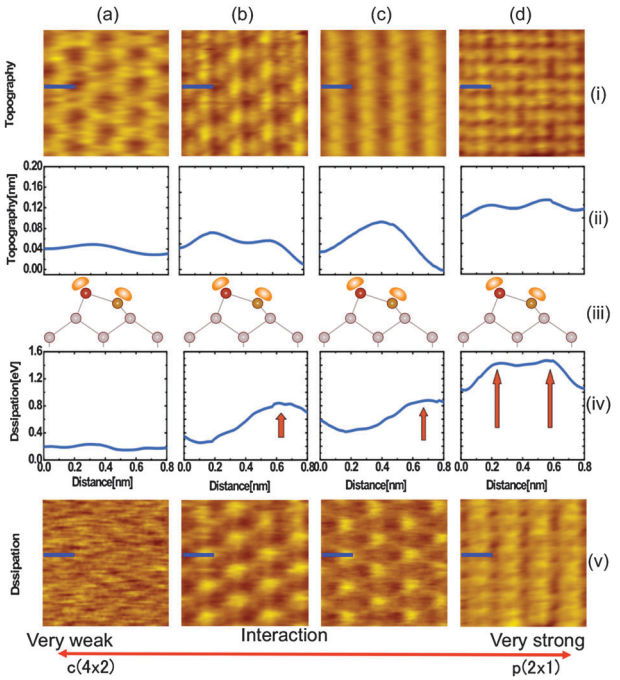

Fig. 8 NC-AFM topographic (i, ii) and corresponding dissipation (iv, v) images and scan lines (taken across the blue line in the images), respectively, of the Si(001) surface taken at 5 K, with a cartoon depicting the cross-section of surface on which the scan line is taken (iii). Scans of the same area were made sequentially without a change of tip apex, at frequency shift Δf values of −10 Hz (a), −20 Hz (b), −22 Hz (c), and −30 Hz (d). Red arrows indicate where significant dissipation is measured. The directions in which strength of the tip–sample interaction changes is schematically indicated at the bottom.

atom in the topography scan line, whereas the lower dimer atom is imaged in the dissipation signal. This means that the contrast in the dissipation image shows an inversion to that in the topography, corresponding to the tip interacting to the lower dimer atom of the surface upon its approach, resulting in the dimer flipping.[25,26]

Interestingly, when the tip–sample interaction becomes stronger, Fig. 8(c), bright lines along dimer rows with flicker noise (due to flipping of surface dimer atoms induced by the tip–sample interaction) are observed in the topographic image,[24] where an average of both dimer atoms is observed in the corresponding scan line. In the dissipation image, however, the $c(4 \times 2)$ phase is still observed; one can also see that dissipation increases above the lower dimer atom trough, indicating that the lower dimer atom *region* is imaged rather than the lower dimer atom alone. This is rather unusual behavior, where completely different image patterns were resolved simultaneously in topographic and dissipation images; the observed contrast in the dissipation image strongly differs from that in topography.

Finally, in the case of very strong tip–sample interaction, Fig. 8(d), the $p(2 \times 1)$ phase is observed in both topographic and dissipation images. Most remarkably, in comparison to the other scan lines, there is another sharp increase in the signal intensity, and dissipation of $\approx$1.4 eV p/o is observed above *both* dimer atoms.

Although direct comparison between experiment and theory may be misleading as the actual tip model is unknown, we note

that the dimer tip model has a promise of delivering closer agreement with experiment in the current case than the stiff pyramidal tip. For instance, experimental dissipation was observed to initially increase above the lower dimer atom by a little more than 0.1 eV, before finally increasing by a further 1.1 eV. Comparing the results obtained with the dimer tip we find not only the qualitative agreement, but also quantitative, as initially dissipation increased by 0.1 eV, before a further 1 eV increase. Also, the absolute value of the dissipation energy observed (around 1.4 eV) is much closer to the value calculated with the dimer tip (just over 1.0 eV) than with the pyramidal tip (over 3.0 eV).

In summary, these experimental results confirm that dissipation does indeed initially occur over the lower dimer atoms, spreading over the entire lower dimer region at smaller tip–sample separations. They appear to agree with our theoretical predictions that dissipation increases in a fairly discontinuous manner (jumps in magnitude) between different Δf values at different lateral positions. They also demonstrate that huge dissipation, well in excess of 1 eV, may also be measured, and crucially shows that the surface atomic structure and contrast patterns in topographic and dissipation images strongly depend on the tip–sample interaction and may differ for the same frequency shift as in Fig. 8(c). In the theoretical topography line scans obtained with the stiff tip, inset in Fig. 3(c), the general trend observed in our experiment, Fig. 8, is correctly predicted, apart from very close separations where, at variance with experimental observations, only one peak is visible for the two dimer atoms. We believe this is most likely related to the crude tip model used, so that a full calculation with the bigger tip would be highly desirable. Unfortunately, calculation of the full scan line with the much bigger dimer tip is computationally beyond our reach right now.

Conclusions

In conclusion, we report not only the processes, which may lead to extraordinarily large dissipation signals; we detail the complexities of their underlying architectures. We find a complex network of interactions, where increasing numbers of bond formations and destructions are observed as the tip approaches and retracts. Typically the tip interacts with a lower dimer atom, causing the dimer to flip. At smaller separations the newly flipped dimer is forced back into its original conformation as repulsion between the tip and upper dimer atom increases. At this point, several bonds form between the tip and surface dimer. In some cases the tip apex is displaced out of plane with the dimer, freeing the strained atoms beneath it, allowing the dimer to flip back into its flipped orientation. These formed bonds then break upon retraction of the tip, generally leading to very large dissipation. Furthermore, we also predict discontinuous contrast and intensity changes, which are experimentally observed and therefore confirmed. All of these features are due to fully reversible processes involving a single dimer flipping multiple times. These processes, being reversible, result in multiple hysteresis loops on the f–z curves. These hysteresis loops encapsulate different amounts of dissipation, which are measured at different tip–sample separations, increasing as the separation decreases. This causes dissipation signal signatures for a given frequency shift to depend critically on how many of these elementary processes occur, resulting in the contrast and intensity of the measured dissipation to vary widely.

We note that, although our results compare reasonably well with available experimental data for weak to strong tip–sample interaction strengths, our tip models are still relatively simple. For strong tip–sample interactions, a larger more flexible tip model would likely achieve a better description, leading to even softer contact with the surface as indicated by our dimer tip. In particular, at small tip–surface distances, dissipation effects are caused by both the tip and surface, with the relative contributions depending on the stiffness (or softness) of either of them. However, such more realistic tips are computationally very demanding. Of course, a real tip used in actual experiments may well be very different to any theoretical model; moreover, it is likely to be extremely difficult, if at all possible, to find the 'true' tip model for each and every experiment. At the same time we do believe that the general trends revealed in this study will remain qualitatively unchanged for a wide variety of possible tips.

Our calculations correspond to zero temperature. Clearly, the predicted step-like behavior is expected to be smoothed out in a room temperature experiment by thermal motion:[3,6,13,16,39] since thermally activated jumps occur even with a barrier present, and this stochastic behaviour would be statistically averaged over several hundred oscillations, steps in the dissipation spectroscopy curves would appear smoother[3] in comparison with those predicted by the zero temperature theory; the magnitude of the dissipation signal would also be reduced.[3,39] Moreover, even at 5 K this smoothing out effect is to be expected as well, albeit in a lesser extend, as every measured point corresponds to averaging over hundreds of tip oscillations, and each of those oscillation cycles will be slightly different than the other.

The results presented here provide an extremely detailed, although *qualitative*, understanding of dissipation on the Si(001)-$c(4 \times 2)$ surface at low temperatures. We hope this work will stimulate further research into atomistic processes happening during NC-AFM imaging approaching the near-contact regime.

Acknowledgements

This work was supported in part by a Grant-in-Aid for Scientific Research of Japan. We acknowledge financial support from the Engineering and Physical Sciences Research Council (EPSRC) and J.B. and S.J. in particular thanks EPSRC for studentship funding. We also acknowledge the support of King's College London's HPC Factility managed by Dr Alessio Comisso and of the University of Nottingham High Performance Computing (HPC) Facility. We thank Material Chemistry Consortium (MCC) for the computer time allocation on the HECToR UK National Facility. We also thank Adam Foster, Adam Sweetman and Alexis Baratoff for helpful comments and discussion.

References

1 R. Hoffmann, A. Baratoff, H. J. Hug, H. R. Hidber, H. v. Löhneysen and H.-J. Güntherodt, *Nanotechnology*, 2007, **18**, 395503.
2 P. M. Hoffmann, S. Jeffery, J. B. Pethica, H. O. Özer and A. Oral, *Phys. Rev. Lett.*, 2001, **87**, 265502.

3 L. Kantorovich and T. Trevethan, *Phys. Rev. Lett.*, 2004, **93**, 236102.
4 A. Schirmeisen and H. Hölscher, *Phys. Rev. B: Condens. Matter Mater. Phys.*, 2005, **72**, 045431.
5 N. Oyabu, P. Pou, Y. Sugimoto, P. Jelinek, M. Abe, S. Morita, R. Pérez and O. Custance, *Phys. Rev. Lett.*, 2006, **96**, 106101.
6 S. A. Ghasemi, S. Goedecker, A. Baratoff, T. Lenosky, E. Meyer and H. J. Hug, *Phys. Rev. Lett.*, 2008, **100**, 236106.
7 L. Kantorovich, M. Gauthier and M. Tsukada, *Noncontact Atomic Force Microscopy*, Springer, New York, 2002.
8 L. Kantorovich and T. Trevethan, *Fundamentals of Friction and Wear on the Nanoscale*, Springer, New York, 2007.
9 H. N. Pishkenari and A. Meghdari, *Physica E*, 2010, **42**, 2069.
10 F. F. Canova and A. S. Foster, *Nanotechnology*, 2011, **22**, 045702.
11 F. J. Giessibl, M. Herz and J. Mannhart, *Proc. Natl. Acad. Sci. U. S. A.*, 2002, **99**, 12006.
12 N. F. Martinez and R. Garcia, *Nanotechnology*, 2006, **17**, S167.
13 M. Watkins, T. Trevethan, A. L. Shluger and L. Kantorovich, *Phys. Rev. B: Condens. Matter Mater. Phys.*, 2007, **76**, 245421.
14 T. Trevethan, M. Watkins, L. Kantorovich and L. Shluger, *Phys. Rev. Lett.*, 2007, **98**, 098101.
15 T. Trevethan, M. Watkins, L. Kantorovich, L. Shluger, J. Polesel-Maris and S. Gauthier, *Nanotechnology*, 2006, **17**, 5866.
16 Y. Sugimoto, P. Pou, O. Custance, P. Jelinek, M. Abe, R. Perez and S. Morita, *Science*, 2008, **322**, 413.
17 S. Kawai, F. F. Canova, T. Glatzel, A. S. Foster and E. Meyer, *Phys. Rev. B: Condens. Matter Mater. Phys.*, 2011, **84**, 115415.
18 R. J. Hamers, R. M. Tromp and J. E. Demuth, *Phys. Rev. B: Condens. Matter Mater. Phys.*, 1986, **34**, 5343.
19 R. A. Wolkow, *Phys. Rev. Lett.*, 1992, **68**, 2636.
20 P. Bokes, I. Štich and L. Mitas, *Chem. Phys. Lett.*, 2002, **362**, 559.
21 Y. Naitoh, Y. J. Li, H. Nomura, M. Kageshima and Y. Sugawara, *J. Phys. Soc. Jpn.*, 2010, **79**, 013601.
22 T. Uda, H. Shigekawa, Y. Sugawara, S. Mizuno, H. Tochihara, Y. Yamashita, J. Yoshinobu, K. Nakatsuji, H. Kawai and F. Komori, *Prog. Surf. Sci.*, 2004, **76**, 147.
23 K. Sagisaka and D. Fujita, *Phys. Rev. B: Condens. Matter Mater. Phys.*, 2005, **71**, 245319.
24 Y. J. Li, H. Nomura, N. Ozaki, Y. Naitoh, M. Kageshima, Y. Sugawara, C. Hobbs and L. Kantorovich, *Phys. Rev. Lett.*, 2006, **96**, 106104.
25 L. Kantorovich and C. Hobbs, *Phys. Rev. B: Condens. Matter Mater. Phys.*, 2006, **73**, 245420.
26 A. Sweetman, S. Jarvis, R. Danza, J. Bamidele, S. Gangopadhyay, G. A. Shaw, L. Kantorovich and P. Moriarty, *Phys. Rev. Lett.*, 2011, **106**, 136101.
27 A. Sweetman, S. Jarvis, R. Danza, J. Bamidele, L. Kantorovich and P. Moriarty, *Phys. Rev. B: Condens. Matter Mater. Phys.*, 2011, **84**, 085426.
28 N. Suehira, Y. Tomiyoshi, Y. Sugawara and S. Morita, *Rev. Sci. Instrum.*, 2001, **72**, 2971.
29 T. Albrecht, P. Grütter, D. Horne and D. Rugar, *J. Appl. Phys.*, 1991, **69**, 668.
30 J. M. Soler, E. Artacho, J. D. Gale, A. García, J. Junquera, P. Ordejón and D. Sánchez-Portal, *J. Phys.: Condens. Matter*, 2002, **14**, 2745.
31 J. P. Perdew, K. Burke and M. Ernzerhof, *Phys. Rev. Lett.*, 1996, **77**, 3865.
32 R. Pérez, I. Štich, M. Payne and K. Terakura, *Phys. Rev. B: Condens. Matter Mater. Phys.*, 1998, **58**, 10835.
33 N. Martsinovich and L. Kantorovich, *Phys. Rev. B: Condens. Matter Mater. Phys.*, 2008, **77**, 205412.
34 H. C. Hamaker, *Physica*, 1937, **4**, 1058.
35 J. Israelachvili, *Intermolecular and Surface Forces*, Academic Press, London, 2nd edn, 1992.
36 J. Bamidele, Y. Kinoshita, R. Turanský, S. H. Lee, Y. Naitoh, Y. J. Li, Y. Sugawara, I. Štich and L. Kantorovich, *Phys. Rev. B: Condens. Matter Mater. Phys.*, 2012, **86**, 155422.
37 Y. Naitoh, Y. Kinoshita, Y. J. Li, M. Kageshima and Y. Sugawara, *Nanotechnology*, 2009, **20**, 264011.
38 S. Jarvis, A. Sweetman, J. Bamidele, L. Kantorovich and P. Moriarty, *Phys. Rev. B: Condens. Matter Mater. Phys.*, 2012, **85**, 235305.
39 T. Trevethan and L. Kantorovich, *Nanotechnology*, 2006, **16**, S205.